Energy Technology
Generation, Conversion, Storage, Distribution
www.entechnol.de

Technoeconomic Analysis of a Fixed Bed System for Single/Two–Stage Chemical Looping Combustion

*Claudio Tregambi, Piero Bareschino, Dawid P. Hanak, Erasmo Mancusi, and Francesco Pepe**

Chemical looping combustion (CLC) is a promising carbon capture technology allowing integration with high-efficiency Brayton cycles for energy production and yielding a concentrated CO_2 stream without requiring air separation units. Recently, dynamically operated fixed bed reactors have been proposed and investigated for CLC. This study deals with the technoeconomic assessment of a CLC process performed in packed beds. Following a previously published work on the topic, two different configurations are considered: one relying on a single oxygen carrier (Cu/CuO based) and the other on two in–series oxygen carriers (Cu/CuO based first, Ni/NiO based later). For both configurations, relevant process schemes are devised to obtain continuous power generation. Despite slightly larger capital costs, two-stage CLC performs better in terms of efficiency, levelized cost of electricity, and avoided CO_2 costs. Fuel price and high–temperature valves costs are identified as the main variables influencing the economic performance. The use of two in–parallel packed bed reactors (2.0 m length, 0.7 m internal diameter) enables a power output of 386 kW_e, a net electric efficiency of 37.2%, a levelized cost of electricity of 91 € MWh_e^{-1}, and avoided CO_2 costs of 55 € ton_{CO2}^{-1} with respect to a reference pulverized coal power plant.

1. Introduction

Carbon dioxide has been widely recognized as one of the main contributors to global warming. Emissions of CO_2 have largely increased in the last decades due to anthropogenic activities, with cement and energy production being two major CO_2 emitting industries. Despite the progress in utilization and integration of renewable energies, carbon capture and utilization/storage (CCUS) technologies are expected to play a key role in reducing the environmental burden of the power industry. CCUS technologies produce a concentrated CO_2 stream ready for subsequent sequestration (e.g., in depleted oil/gas reservoirs or deep saline formations[1]) or utilization (e.g., in methanation processes[2]). CCUS technologies are generally distinguished in post–, pre–, and oxy–combustion. Postcombustion techniques, such as calcium looping, have the advantage of being retrofittable to already existing power plants, but may require the use of an expensive air separation unit, if not integrated with renewable energies (e.g., concentrated solar thermal[3]). Conversely, pre- and oxy–combustion technologies require major adjustments to the existing power plants or the design of new kind of power plants.

Chemical looping combustion (CLC) is a promising combustion technology that avoids the need for an expensive air separation unit. It also allows integration with high-efficiency Brayton cycles for energy production. In CLC, fuel and air are indirectly contacted by means of an intermediate solid compound, so-called oxygen carrier (OC), and the combustion process is split in a two-step process.[4–6] The OC is a metal oxide compound made of an active phase able to reversibly exchange oxygen (e.g., Cu/CuO, Ni/NiO, $Fe_2O_3/Fe_3O_4/FeO$), supported on an inert material (e.g., Al_2O_3, ZrO_2) required to improve the mechanical and chemical–physical properties (e.g., porosity, kinetics) of the solid particles.[7,8] In the first stage of CLC, the OC reacts with the fuel by providing the O_2 required for the chemical reaction. As a result of fuel oxidation, a stream of H_2O and CO_2 is produced, while the OC is converted into a reduced form. Following the sensible heat recovery and steam condensation, a pure CO_2 stream is obtained. Depending on the OC/fuel couple, this stage can be either endothermic or exothermic. In the second step, the OC reacts with the O_2 in the air and is oxidized to its original state. At the same time, a stream of O_2–lean air is produced. This stage is always exothermic. The produced high–temperature gas stream is fed to a gas turbine for power generation. It is worth noting that CLC may be used for processing of solid fuels (e.g., coal, biomass) via in situ[9] or external pregasification.[10–13]

As CLC involves gas–solid chemical reactions, the use of two interconnected fluidized beds, one acting as a fuel reactor and the other as an air reactor, has been extensively explored in the

C. Tregambi, P. Bareschino, E. Mancusi, F. Pepe
Dipartimento di Ingegneria
Università degli Studi del Sannio
Piazza Roma 21, 82100 Benevento, Italy
E-mail: francesco.pepe@unisannio.it

D. P. Hanak
Energy and Power, School of Water, Energy and Environment
Cranfield University
Cranfield, Bedfordshire MK43 0AL, UK

The ORCID identification number(s) for the author(s) of this article can be found under https://doi.org/10.1002/ente.202100538.

DOI: 10.1002/ente.202100538

literature.[14–19] However, it has been estimated that to improve the competitiveness of CLC, the stream fed to the gas turbine must feature very high temperature (≈1473 K) and pressure (20–30 bar).[20–22] This poses significant challenges for the operation of fluidized bed reactors because of both the high–pressure operation and the efforts required for the gas–solid separation at high temperature/pressure. Elutriated fines present in the outlet stream can negatively impact the performance and durability of the downstream gas turbine. Moreover, environmental and safety concerns have been posed regarding the potential release of trace elements of OCs based on hazardous metallic oxides (e.g., Ni).[23] To circumvent such problems, Noorman et al. proposed[21] and experimentally investigated[22] the use of dynamically operated fixed bed reactors. In a packed bed, the OC particles are stationary and are alternately exposed to reducing and oxidizing conditions through a periodic switching of the feed conditions. In contrast to fluidized beds, fixed beds may suffer from inefficient heat/mass transfer that could lead to the formation of hot spots.[24] However, fixed beds are more easily operated at the high pressures required for subsequent gas turbine expansion of exhaust gas. Moreover, gas/solid separation is intrinsically achieved, and problems related to attrition/elutriation of the OC are reduced. Given the intrinsic intermittent nature of fixed beds, a network entailing multiple parallel reactors is required to ensure continuous power generation.

As being first proposed for CLC, several studies have been performed that focused mainly on multiple arrangements of fixed beds and proper control and optimization of heat management. Spallina et al.[12,20] investigated the use of different strategies for heat management in a packed bed reactor, considering ilmenite as OC and syngas from coal gasification as fuel. They demonstrated the potentials of the packed bed reactor technology of working under high-pressure conditions, and the possibility of producing a pressurized hot gas stream at almost constant operating conditions, which can be easily coupled with an efficient thermodynamic cycle for energy generation. Fernandez and Abanades[25] modeled a system of eight in–parallel fixed bed reactors using Ni-based materials as OC and natural gas as fuel. A preliminary design of a reactor network able to process a mass stream of 20 kg s^{-1} of methane was performed, identifying reasonable operating conditions and confirming the technical feasibility and large potential of the fixed-bed reactor technology applied to CLC. Ortiz et al.[26] synthesized, and experimentally tested in a packed bed reactor, ilmenite particles with different shapes and compositions, focusing on the mechanical properties of the particle during iterated thermal/chemical cycling. Similar experiments were also performed by Jacobs et al.[27] It was found that the additive used in the synthesis has an important effect on the mechanical properties of the pellets. Granules were identified as a promising shape for packed bed reactors because no severe degradation in strength was detected upon thermal cycling and creep testing. Mn_2O_3 was found to be the best additive for ilmenite–based granules. Hamers et al.[28] performed experimental tests under pressurized conditions to scrutinize the effect of the pressure on kinetics, using CuO/Al_2O_3 and $NiO/CaAl_2O_4$ as OCs. According to their results, increasing the pressure has a twofold effect on the overall reaction rate: on one hand, it induces a small decrease in the kinetics because of a reduced number of oxygen vacancies; on the other hand, it has a positive effect because of the decrease in the internal diffusion limitations. Han and Bollas[29] explored the possibility of periodically reversing the gas flow direction in the packed bed to improve the uniformity in concentration and temperature profiles within the bed. It was found that periodic reversal of the flow during the reduction step improves the contact between the fuel and unconverted OC, suppressing unwanted catalytic reactions and axial conversion/temperature gradients. A similar strategy was investigated by Hamers et al.[11] However, their study reported more severe temperature fluctuations in the reactor exhaust gas that is an unfavorable scenario for the downstream gas turbine operation. Lucio and Ricardez-Sandoval[30] investigated, using a 1D heterogeneous model, optimal control strategies targeted at enhancing heat recovery and reducing fuel slip during oxidation/reduction steps. Their results showed a high degree of heat recovery and a near-complete methane conversion into CO_2 and H_2O, supporting the importance of the CLC in packed bed reactors.

An additional challenge in the operation of fixed bed reactors is that the OC should experience a considerable temperature rise to reach the high temperatures required to boost the overall process efficiency (from about 723–823 to 1473 K). Despite being thermodynamically feasible, for some materials this would require the synthesis of an OC with a substantial fraction of active phase, whose chemical and mechanical stability over iterated cycles would be a matter of concern. For this reason, Hamers et al.[10,11] proposed and modeled a two–stage CLC process, in which the overall temperature rise is split among two in–series OCs. In their work, they investigated the performance of a CLC plant coupled with an integrated gasification combined cycle, in which the first OC is based on Cu and the second OC is based on Mn. Subsequent experimental studies were also performed by Kooiman et al.[31] using CuO/Al_2O_3 and $NiO/CaAl_2O_4$ in series, confirming the viability of this approach. More recently, Mancusi et al.[32] analyzed CLC of methane and compared the performance of a single fixed bed reactor in a configuration embodying either one or two in–series OCs. Transient material and energy balance equations were solved to evaluate the composition and temperature of the different streams exiting the reactor during the process. The use of two in-series OCs allowed obtaining higher temperature for the stream fed to the gas turbine, with expected higher plant efficiencies and performances. The overall temperature increase of about 600 K from inlet to outlet conditions was equally split between the two carriers, thus enhancing the reliability of the system. However, the economic feasibility of using two in-series OCs as opposed to a single OC has not yet been assessed.

This study builds on the modeling work by Mancusi et al.[32] and aims to perform a comprehensive technoeconomic analysis of the fixed bed CLC process. It considers two CLC configurations based on a single and two in-series OCs. For each of the considered configurations, a specific scheme embodying multiple in–parallel fixed bed reactors was designed to achieve a continuous power generation at the gas turbine. Energy consumption and production of the key components of the reactor network was assessed to evaluate the actual energy produced and the overall energy conversion efficiency. An economic analysis was then performed to estimate the levelized cost of electricity (LCOE) and the avoided CO_2 costs (ACC) for both

configurations. Finally, sensitivity analysis and a net present value analysis were performed to complete the technoeconomic assessment.

2. Design of the Reactor Scheme

This section describes the layout devised for the two reactor configurations investigated (i.e., single OC, also referred as single–stage, and two in–series OCs, also referred as two–stage).[32] When CLC is performed in a fixed bed system, the different steps of the process (e.g., reduction, oxidation) are sequentially performed within the reactor. Given the intrinsic transient nature of fixed beds, a reactor network including multiple in–parallel reactors must be designed to allow for continuous power generation or processing a continuous reactant stream. Typically, the different steps required by CLC in fixed beds are as follows[11,20]: 1) oxidation step (OS): a stream of air reacts with the reduced form of the OC. The temperature of the solid phase increases due to the exothermicity of the chemical reaction. The OC is converted into its oxidized form and exhaust gas consists of O_2–depleted air; 2) heat recovery after oxidation step (HROS): a stream of air is sent into the fixed bed reactor to remove the heat accumulated by the solid carrier because of the OS. No chemical reaction occurs. Exhaust gas consists of air at a higher temperature, sent to the turbine for expansion and energy production; 3) purge step (PS): a stream of N_2 is used to "wash" the reactor and reduce the O_2 concentration inside the reactor; 4) reduction step (RS): a gaseous fuel is fed to the fixed bed reactor to reduce the OC. A stream of CO_2 and H_2O leaves the reactor, and the OC is converted to its reduced form. The reaction can be exothermic or endothermic, therefore the temperature of the solid carrier may increase or decrease, depending on the chemical nature of the OC and the fuel used; 5) purge step (PS) or heat removal after reduction step (HRRS): a stream of N_2 is used to wash the reactor and reduce the fuel concentration inside the reactor (PS). If required by the system's constraints, heat is also removed during this step by the N_2 stream (HRRS) so that the temperature of the solid carrier during the subsequent oxidation step does not increase over a threshold value.

2.1. Methodology

Depending on the desired output, different strategies can be implemented for the design of the reactor network. Hamers et al.[24] studied the integration of CLC in a fixed bed with a gasification system and designed the reactor scheme to process the continuous syngas stream exiting the gasification unit. In this study, the CLC of methane is considered. The reactor network was designed by considering that a constant energy production at the gas turbine should be obtained. In other terms, at least one reactor should always be in HROS. In this way, the system may be conceived to operate as a baseload power plant. The reactor network was designed with the further goals of keeping the capital/investment costs as low as possible, thus arranging the minimum number of reactors in parallel, and ensuring a constant gas flow rate through the gas turbine to avoid the need for gas buffers. To fulfill these targets, it should be verified that

$$\frac{t_{HROS}}{t_{TOT}} \cdot N_R = 1 \tag{1}$$

where t_{HROS} is the time required for the HROS, t_{TOT} is the duration of a whole cycle of CLC, and N_R is the number of reactors operating in parallel in the network. As N_R is an integer and the ratio between t_{HROS} and t_{TOT} is clearly lower than 1, the minimum number of parallel reactors is 2. For this to occur, it is required that the duration of the HROS is half of the whole cycle length. The design of the reactor network was performed considering the following assumptions: 1) compression/expansion can be modeled as single-stage reversible process[10,20]; 2) heat exchange between the different streams entering/leaving the system can be performed using adiabatic thermal buffers. A temperature difference of at least 25 K between the stream entering and leaving the buffer is required to ensure efficient heat transfer.

2.2. Process Description: Single OC

Main operating conditions and results of the CLC process based on a single OC, and investigated in the previous work,[32] are briefly presented. The CLC of CH_4 was performed using Cu/CuO as the active phase of the OC. Cu-based OCs have good oxygen transport capacity, an appreciable lifetime, and high reaction rates even at low temperatures. However, due to the low melting temperature, these OCs cannot be used above 1200–1300 K.[23] Therefore, a Cu-based OC represents a good choice for the single carrier configuration with a moderate operating temperature. Inlet and outlet temperatures, inlet mass fluxes, and period lengths are shown in **Table 1** for the different steps of the process. Within the operational conditions investigated, it was necessary to partly remove the heat accumulated after the reduction step (HRRS is performed instead of PS) to avoid the sintering of the OC during the subsequent exothermal oxidation step. A stream of hot air at about 1173 K and 19.7 bar is produced during the HROS and expanded in a turbine for power generation.

For data shown in Table 1, a value of 0.47 is obtained for the ratio between t_{HROS} and t_{TOT}, very close to the 0.5 value for which simply two in–parallel reactors would be needed. Operating conditions were then slightly tuned to obtain a ratio of 0.5. This was achieved by decreasing the period of the HRRS to 805 s and, correspondingly, increasing the inlet mass flux to 2.6 $kg\,m^{-2}\,s^{-1}$. The feasibility of this modification was verified with new model computations. As no significant differences were detected in the main results (see Supporting Information), the tuned operating conditions, which simply require the use of two in–parallel reactors, were used to design the reactor network. The sequence of

Table 1. Main data of the CLC process, single carrier configuration.

Stage	Temperature [K]		Inlet mass flux [$kg\,m^{-2}\,s^{-1}$] (tuned value)	Period [s] (tuned value)
	Inlet	Average outlet		
OS	850	850	2	320
HROS	850	1173	2	1610
PS	850	988	6	170
RS	850	850	0.133	315
HRRS	850	1015	2 (2.6)	1040 (805)

steps taking place in the two reactors under tuned conditions is shown in **Figure 1**, with a delay of operation between them equal to half the whole cycle length (equivalent to the HROS period). As can be seen, the different steps never overlap, and continuity of the HROS is ensured. **Figure 2** shows the process scheme designed for the CLC operation. Thermal buffers, turbine, and compressors are shared between the two reactors. Temperature values detailed in the sketch are obtained based on the considerations made in the previous section. Starting with the OS, the air is compressed up to 20 bar and sent into thermal buffer #1 for preheating. As the outlet temperature is lower than that required by initial conditions (i.e., 850 K; see Table 1), an auxiliary heater powered by the electrical energy produced by the reactor network is required to complete preheating. The air stream is then sent to the fixed bed reactor, where oxidation of the OC occurs. Exhaust gas, consisting of high-pressure nitrogen at 850 K, is "recycled" in the parallel fixed bed, which at that time is performing the HROS (see Figure 1). When the OC is almost completely oxidized, the OS step ends and the HROS begins. Input stream to the reactor does not change, but exhaust gas, consisting of high temperature/pressure air, is sent to the gas turbine where it is expanded for power generation. To increase the power generation of the reactor network, exhaust air from gas turbine is eventually exploited in a bottoming steam cycle, whose description is provided in Section 2.4. After the HROS, a short PS is performed. Compressed N_2 is preheated into thermal buffer #2 up to 850 K and then sent to the fixed bed. The "impure" exhaust N_2, hotter than its entrance because of the residual heat accumulated by the OC, is sent to thermal buffer #2 for heat recovery. Once the fixed bed is flushed from oxygen, RS begins. To this end, a stream of methane is compressed up to 20 bar and sent into thermal buffer #3 for preheating. As for the air stream, an auxiliary heater is required to reach the set inlet temperature. Methane is then sent into the packed bed reactor to reduce the OC. The exhaust stream, consisting of a mixture of CO_2 and H_2O, is sent into thermal buffer #3 for heat recovery, and then exploited in the bottoming steam cycle where, upon heat recovery, CO_2 is eventually sent to storage. Finally, an HRRS is performed to close the CLC cycle. A stream of compressed nitrogen is preheated into thermal buffer #4 up to 850 K and sent to the fixed bed for both flushing of residual fuel and reducing the OC temperature before the OS. Exhaust gas, consisting of hot "impure" nitrogen, is sent in–series to thermal buffers #1 and #4 for heat recovery.

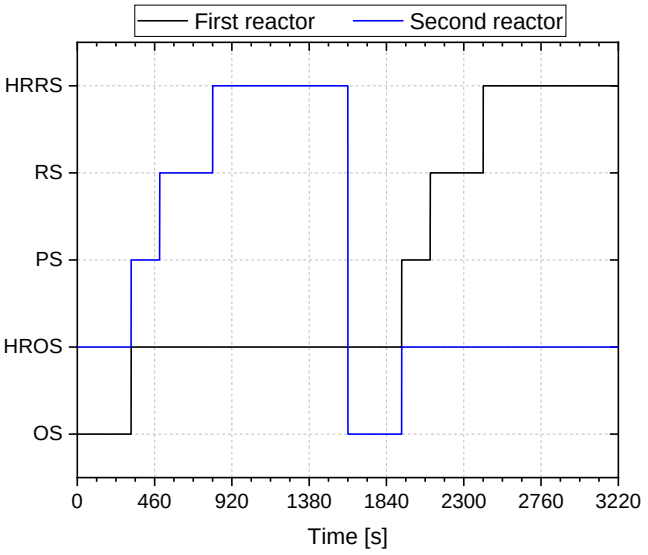

Figure 1. A sequence of operation for the two parallel reactors, single carrier configuration.

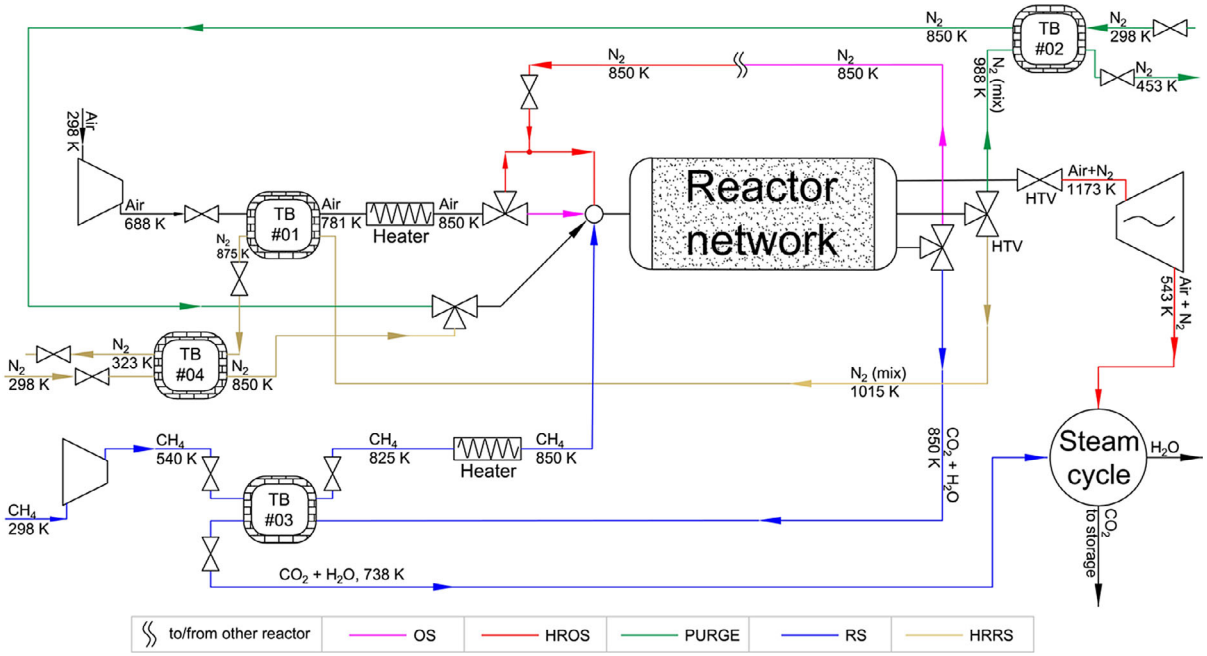

Figure 2. Sketch of the reactor network, single carrier configuration.

The design of the reactor scheme for the single carrier configuration shows that heat recovered from the outlet gas streams is not sufficient for a complete preheating of the reactant streams. Therefore, a part of the electrical energy produced by the system needs to be used to power the auxiliary heaters and ensure preheating the reactant streams.

2.3. Process Description: Two in–Series OCs

Main operating conditions and results of the CLC process based on two in–series carriers (two–stage CLC), and investigated in the previous study,[32] are briefly presented. CH_4 was considered as fuel, and the OCs were based on Cu/CuO and Ni/NiO. Ni-based OCs, though being more expensive, show a very high reactivity and good performance even at high temperature (1473 K). In the two carriers configuration, the first bed section is responsible for the first temperature rise, while the second bed is responsible for the remaining temperature rise, demanding that the OC should be able to withstand higher temperatures. Consequently, Cu/CuO as the first OC ensures fast kinetics at low temperature and lower capital costs, while Ni/NiO as the second OC allows to strongly increase the final process temperature, leading to a higher power generation at the turbine. Inlet and outlet temperatures, inlet mass fluxes, and period lengths are shown in **Table 2** for the different steps of the process. For data in Table 2, the ratio between t_{HROS} and t_{TOT} equals 0.51. As for the single carrier configuration, operating conditions were slightly tailored to have a ratio of 0.5. In addition, inlet mass flux during the two purge steps was slightly reduced to increase the length of the stage. The feasibility of this modification was confirmed by specific model simulations (see Supporting Information). Therefore, as for the single carrier configuration, the use of two in–parallel reactors can ensure continuous power generation at the turbine.

A sequence of steps undergoing in the two reactors is shown in **Figure 3**, with a time delay between their operation always set at half the whole cycle. Figure 3 confirms that different steps never overlap and that continuity of the HROS is maintained. **Figure 4** shows the process scheme designed for the system operation. Starting with the OS, ambient air is compressed up to 20 bar and sent in–series to thermal buffer #1 and thermal buffer #2, where it is preheated up to a temperature of 850 K. The preheated air stream enters the fixed bed reactor to perform the OS, increasing the temperature of the solid material. The high pressure/temperature stream of N_2 leaving the reactor is first fed to thermal buffer #1 for heat recovery, and then recycled into the parallel reactor for the HROS (see Figure 3). Once oxidation of the carrier is complete, the OS is arrested and the HROS starts.

Table 2. Main data of the CLC process, two carriers configuration.

Stage	Temperature [K]		Inlet mass flux [kg m^{-2} s^{-1}] (tuned value)	Period [s] (tuned value)
	Inlet	Average outlet		
OS	850	1150	2	195
HROS	850	1473	2	470
PS (1)	850	1378	6 (4.2)	30 (42.5)
RS	850	850	0.133	190
PS (2)	850	1173	6 (4.2)	30 (42.5)

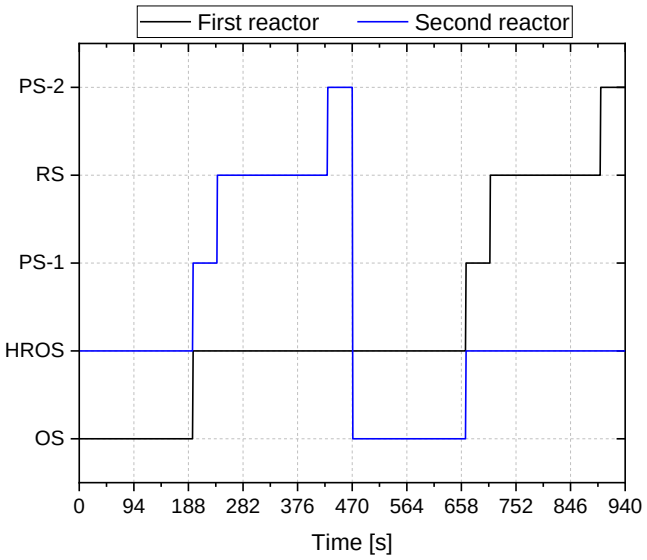

Figure 3. Sequence of operation for the two parallel reactors, single carrier configuration.

During this stage, input stream to the reactor is unchanged, but exhaust gas, consisting of high temperature/pressure air, is sent to the gas turbine for power generation. Similar to the previous process scheme (see Figure 3), exhaust air from gas turbine is exploited in a bottoming steam cycle to increase the power generation of the reactor network. When most of the useful heat has been removed from the solid material, the HROS is arrested and a short PS is performed to flush the oxygen from the reactor before the fuel is supplied. To this end, a stream of compressed nitrogen is sent to thermal buffer #3 for preheating up to 850 K and then fed to the reactor. Exhaust gas, consisting of hotter impure nitrogen because of the heat still accumulated by the solid material, is returned back to thermal buffer #3 for heat recovery. For the RS, a stream of methane is compressed up 20 bar, preheated up to 850 K into thermal buffer #4, and fed to the fixed bed reactor. The stream leaving the system, consisting of a mixture of H_2O and CO_2 at high temperature, is sent in–parallel to thermal buffer #2 and #4 for heat recovery and then exploited in the bottoming steam cycle where, upon heat recovery, CO_2 is eventually sent to storage. Lastly, a final PS is performed to flush the reactor from the residual fuel before starting a new cycle. Preheating of the nitrogen stream and recovering of the exhaust gas sensible heat are performed as for the previous PS.

Overall, in contrast to the single carrier configuration and under the considered operational conditions, two-stage CLC does not require removal of heat after the reduction step (PS is performed instead of HRRS). As a result, the whole cycle length is shorter (940 vs 3220 s), and the temperature of the gas stream fed to the gas turbine is much higher (1473 vs 1173 K), as well as those of the CO_2/H_2O stream (924 K vs 738 K) and of the exhaust air stream (703 vs 543 K) fed to the steam cycle. Moreover, a comparison between Figure 2 and 4, and the relative process description presented earlier, highlights an important difference between the two process schemes. In the two carriers

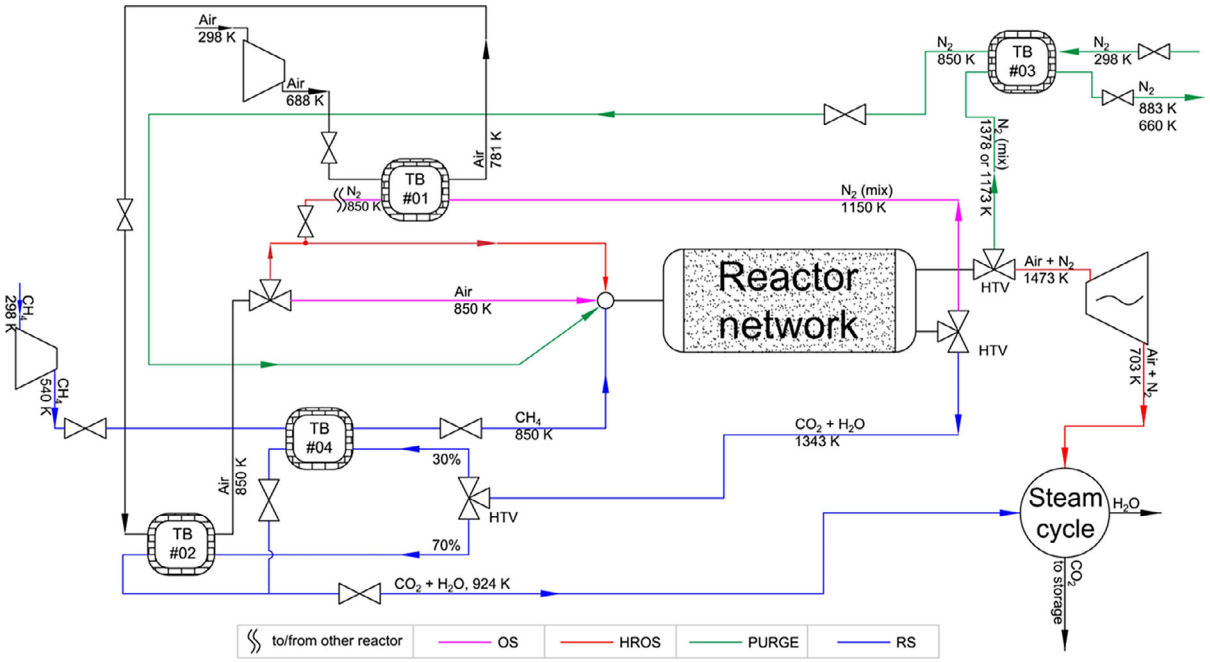

Figure 4. Sketch of the reactor network, two–stage CLC.

configuration, preheating of the reactant streams can be fulfilled by exploiting the sensible heat of the product streams. Therefore, no auxiliary heaters are required, and energy produced at the turbine is fully available.

2.4. Process Description: Bottoming Steam Cycle

To maximize the efficiency of the entire process, the high-grade heat available in the CO_2/H_2O and Air/N_2 streams leaving the CLC is utilized in a bottoming steam cycle. Because the CLC process has been designed to ensure a continuous operation of the expander, the CO_2/H_2O stream is only available for a specific period of time throughout the cycle. This is 19.6% and 40.4% of the operating time for the single- and two-stage CLC, respectively. Therefore, a vessel for intermediate storage of CO_2/H_2O is considered to ensure a continuous operation of the steam cycle.

The considered topology of the bottoming steam cycle is based on the study by Hanak et al.[33] and shown in **Figure 5**. The heat exchanger network is designed in Aveva Process Simulation as a set of three heat exchangers to raise saturated steam. Unsaturated steam is first produced from the feedwater in the evaporators. These heat exchangers were designed for the minimum temperature difference of 25 K. Saturated steam is then produced in the final steam generator that was also designed to operate with the minimum temperature difference of 25 K. To maximize the efficiency of the steam cycle, the steam pressure at the steam turbine inlet was selected considering the minimum temperature difference between the CO_2/H_2O stream temperature and the steam saturation temperature of 10 K. This results in the optimum cycle pressure of 46.8 and 160 bar for single- and two-stage CLC for which the CO_2/H_2O stream temperatures are 738 and 983 K, respectively. The saturated steam is then expanded to the condenser pressure in a steam turbine. The pressure of the condensate is then increased to the maximum cycle pressure in the feedwater pump.

3. Technoeconomic Analysis

3.1. Methodology and Parameters

The following section describes the methodology implemented to estimate the power production of the plant and its efficiency, as well as the capital and operating costs, the LCOE, and the ACC. Values of the main parameters are given along with their discussion, and further shown in **Table 3**.

3.1.1. Energy/power Production

The energy produced at the gas turbine during a whole cycle (E_{GT}) was estimated as

$$E_{GT} = W_{HROS}(h_{GT}^{in} - h_{GT}^{out})t_{HROS}N_R\eta_{GT} \quad (2)$$

where W_{HROS} is the mass stream of air during the HROS, h_{GT}^{in} and h_{GT}^{out} are the enthalpy of the air stream entering and leaving the turbine, respectively, t_{HROS} is the duration of the HROS, and η_{GT} is the overall power–to–electric efficiency of the gas turbine, set at 0.91.[34] The inlet condition of the gas turbine is that of the air stream produced during the HROS. Expansion is performed up to atmospheric pressure, and outlet temperature is estimated by considering a reversible adiabatic expansion (isentropic).

The energy required for the air compression during a whole cycle ($E_{comp,air}$) was estimated as

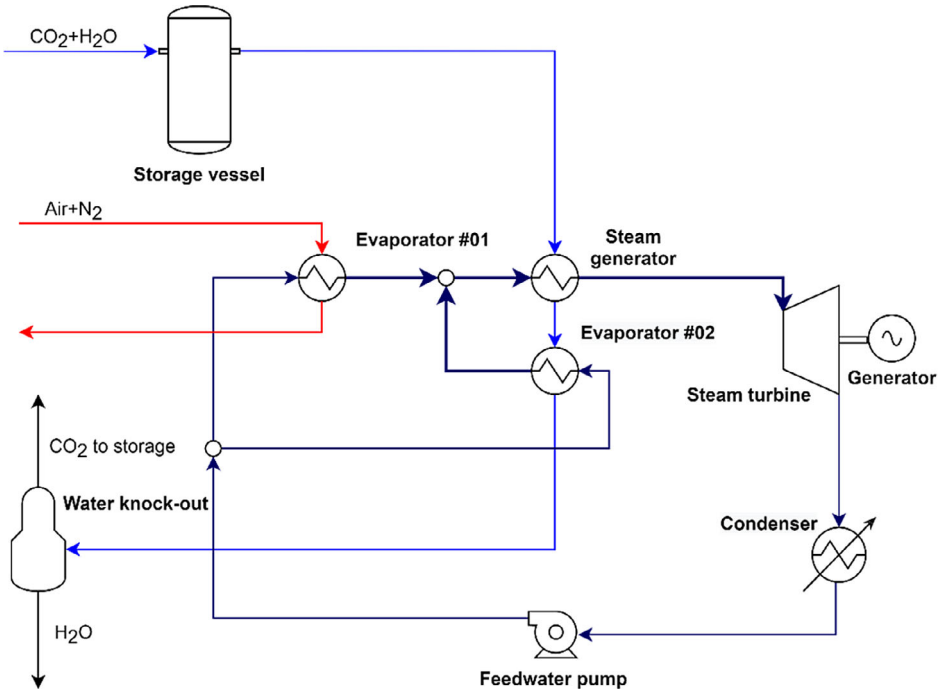

Figure 5. Sketch of the bottoming steam cycle.

Table 3. Main parameters required for the technoeconomic analysis.

Parameter	Symbol	Value	Unit	Reference
Capacity factor	CF	0.85	[–]	[34,37]
Reference cost of the active phase	$C_{ref,ap}$	6000 (Cu) 13 000 (Ni)	[€ ton^{-1}]	–
Reference cost of the inert solid material	$C_{ref,ap}$	1000	[€ ton^{-1}]	[38]
Reference cost of high temperature valve (reference stream of 2 m^3 s^{-1})	$C_{ref,HTV}$	150000	[€]	[10,24]
Reference cost of internal refractory	$C_{ref,refr}$	450	[€ ton^{-1}]	[10,24]
Reference cost of steel	$C_{ref,steel}$	500	[€ ton^{-1}]	[10,24]
Reference cost for transport and storage of CO_2	C_{TS}	10	[€ ton^{-1}]	[37]
External diameter of the packed bed	D	0.7	[m]	[32]
Design stress of steel	f	85	[N mm^{-2}]	[10,24]
Fixed operating maintenance cost	FOM	1% of TCC	[€ year^{-1}]	[34]
Length of the reactor	L	2	[m]	[32]
Expected lifetime of the OC	$lt_{carrier}$	5	[year]	[37]
Expected lifetime of high temperature valves	lt_{HTV}	10	[year]	–
Project interest rate	PIR	8.75	[%]	[34]
Specific fuel cost	SFC	19.1	[€ MW^{-1} h^{-1}]	[38]
Threshold temperature value for the steel vessel	$T_{max,steel}$	573	[K]	[10,24]
Expected lifetime of the CLC plant	γ	25	[year]	[37]
Efficiency of the compressor (isentropic)	η_{comp}	0.87	[–]	[34,35]
Overall power–to–electric efficiency of the gas turbine (isentropic)	η_{GT}	0.91	[–]	[34]
Thermal conductivity of refractory	λ	0.2	[W m^{-1} K^{-1}]	[10,24]

$$E_{\text{comp,air}} = \frac{(W_{\text{HROS}} t_{\text{HROS}} + W_{\text{OS}}^{\text{in}} t_{\text{OS}} - W_{\text{OS}}^{\text{out}} t_{\text{OS}})(h_{\text{comp,air}}^{\text{out}} - h_{\text{comp,air}}^{\text{in}}) N_{\text{R}}}{\eta_{\text{comp,air}}} \quad (3)$$

where $W_{\text{OS}}^{\text{in}}$ and $W_{\text{OS}}^{\text{out}}$ are the inlet mass stream of air and the outlet mass stream of O_2-depleted air, respectively, during the OS, t_{OS} is the length of the OS, and $h_{\text{comp,air}}^{\text{out}}$ and $h_{\text{comp,air}}^{\text{in}}$ are, respectively, the enthalpy of the air stream leaving and entering the compressor. Finally, $\eta_{\text{comp,air}}$ is the efficiency of the air compressor, assumed to be 0.87.[34,35] The equation estimates the energy required by considering that the O_2 depleted air produced during the OS is recycled in the HROS (see Section 2.2 and 2.3).

The energy required for the methane compression during a whole cycle was estimated as

$$E_{\text{comp,meth}} = \frac{W_{\text{RS}}^{\text{in}} (h_{\text{comp,meth}}^{\text{out}} - h_{\text{comp,meth}}^{\text{in}}) t_{\text{RS}} N_{\text{R}}}{\eta_{\text{comp,meth}}} \quad (4)$$

where $W_{\text{RS}}^{\text{in}}$ is the inlet mass stream of methane entering the reactor during the RS, $h_{\text{comp,meth}}^{\text{out}}$ and $h_{\text{comp,meth}}^{\text{in}}$ are, respectively, the enthalpy of the methane stream leaving and entering the compressor, t_{RS} is the period of the RS, and $\eta_{\text{comp,meth}}$ is the efficiency of the methane compressor, set equal to that of the air compressor.

For both air and methane compressors, inlet conditions are ambient temperature (298 K) and atmospheric pressure, whereas outlet conditions are 20 bar and temperature estimated by referring to a reversible single-stage adiabatic compression (isentropic).

The energy required by the auxiliary air heater ($E_{\text{aux,air}}$) was estimated as

$$E_{\text{aux,air}} = (W_{\text{HROS}} t_{\text{HROS}} + W_{\text{OS}}^{\text{in}} t_{\text{OS}} - W_{\text{OS}}^{\text{out}} t_{\text{OS}}) \overline{C_{\text{p,air}}} (T_{\text{HROS/OS}} - T_{\text{air}}^{\text{HR}}) N_{\text{R}} \quad (5)$$

where $T_{\text{HROS/OS}}$ is the temperature of the air stream entering the HROS and OS and $T_{\text{air}}^{\text{HR}}$ is the temperature of compressed air after the heat recovery step.

Finally, the energy required by the auxiliary methane heater ($E_{\text{aux,meth}}$) was estimated as

$$E_{\text{aux,meth}} = W_{\text{RS}} \overline{C_{\text{p,meth}}} (T_{\text{RS}} - T_{\text{meth}}^{\text{HR}}) t_{\text{RS}} N_{\text{R}} \quad (6)$$

where T_{RS} is the temperature of the methane stream entering the RS and $T_{\text{meth}}^{\text{HR}}$ is the temperature of compressed methane after the heat recovery step. It is recalled that auxiliary heaters are required only for the single carrier configuration (see Section 2.2 and 2.3).

The energy produced by the steam turbine in the bottoming steam cycle (E_{ST}) was obtained from computation with Aveva Process Simulation, with main process parameters shown in **Table 4**. A condenser pressure of 0.06 bar was assumed, whereas the isentropic efficiency of the steam turbine and feedwater pump was set at 85% and 80%, respectively. The pressure drop across the heat exchangers was assumed to be 0.5 bar. The overall heat transfer coefficient of 1000, 1500, and 350 $\text{W m}^{-2}\,\text{K}^{-1}$ was assumed for the evaporators, condenser, and steam generator, respectively.[33,36]

Table 4. Main data of the bottoming steam cycle.

Parameter	Value	Reference
Minimum temperature difference of each heat exchanger [K]	25	[33]
Minimum temperature difference for saturated temperature [K]	10	[33]
Condenser pressure [bar]	0.06	[33]
Isentropic efficiency of steam turbine [%]	85	[33]
Isentropic efficiency of feedwater pump [%]	80	[33]

Net electric power produced by the reactor network was estimated as

$$P_{\text{net}} = \frac{E_{\text{GT}} + E_{\text{ST}} - E_{\text{comp,air}} - E_{\text{comp,meth}} - E_{\text{aux,air}} - E_{\text{aux,methane}}}{t_{TOT}} \frac{1}{10^6} \quad (7)$$

Finally, the net efficiency of the system was defined as

$$\eta_{\text{net}} = \frac{P_{\text{net}} t_{\text{TOT}} 10^6}{W_{\text{RS}} \text{LHV}_{\text{meth}} t_{\text{RS}} N_{\text{R}}} \quad (8)$$

where LHV_{meth} is the lower heating value of methane.

3.1.2. Economic Analysis

An economic analysis of the considered processes was performed by estimating capital costs, LCOE, and ACC. LCOE was estimated as

$$\text{LCOE} = \frac{\text{TCC} \cdot \text{FCF} + \text{FOM}}{8760 \cdot \text{CF} \cdot P_{\text{net}}} + \text{VOM} + \frac{\text{SFC}}{\eta_{\text{net}}} \quad (9)$$

where TCC are the total capital costs of the reactor network, FCF is the fixed charged factor, FOM are the fixed operating and maintenance costs, CF is the capacity factor of the plant, set at 0.85,[34,37] 8760 is the average number of hours in a year, VOM are the variable operating and maintenance costs, and SFC is the specific fuel cost, set equal to 19.1 € $\text{MW}^{-1}\,\text{h}^{-1}$ (5.3 € GJ^{-1}).[38] TCC was assessed by estimating the costs of the main components of the reactor network. FCF was estimated as

$$\text{FCF} = \frac{\text{PIR}}{1 - (\text{PIR} + 1)^{-\gamma}} \quad (10)$$

where PIR is project interest rate, set at 8.75%[34] and γ the year of amortization, set equal to the expected lifetime of the plant (25 years).

FOM were assumed to be equal to 1% of TCC per year.[34] VOM were evaluated as the sum of three different contributions

$$\text{VOM} = \text{VC}_{\text{TS}} + \text{VC}_{\text{HTV}} + \text{VC}_{\text{OC}} \quad (11)$$

where VC_{TS} are the variable costs related to the transport and storage of CO_2, VC_{HTV} are the variable cost related to the

maintenance of the high-temperature valves required at the outlet of the fixed bed reactors, and VC_{OC} are the variable costs related to the maintenance of the solid OC. They were estimated as

$$VC_{TS} = W_{RS}^{out}\omega_{CO_2}CF\frac{t_{RS}}{t_{TOT}}\frac{C_{TS}}{P_{net}}N_R\frac{3600}{1000} \quad (12)$$

where W_{RS}^{out} is the outlet mass stream during the RS, ω_{CO_2} is the mass fraction of CO_2 in the outlet stream, and C_{TS} is the specific cost for transport and storage of CO_2, set equal to 10 € ton^{-1}[37]

$$VC_{HTV} = \frac{C_{HTV}}{lt_{HTV}8760\cdot CF\cdot P_{net}} \quad (13)$$

where C_{HTV} is the cost of the high–temperature valves of the reactor network and lt_{HTV} is the lifetime expected for the valves, set equal to 10 years

$$VC_{OC} = \frac{C_{OC}}{lt_{OC}8760\cdot CF\cdot P_{net}} \quad (14)$$

where C_{OC} is the overall cost of the solid material and lt_{OC} is the lifetime expected for the carrier, set equal to 5 years.[37]

Finally, the ACC were estimated as

$$ACC = \frac{LCOE_{CLC} - LCOE_{ref}}{e_{CO_2,ref} - e_{CO_2,CLC}} \quad (15)$$

where $LCOE_{ref}$ is the levelized cost of electricity of a reference combustion system without carbon capture and storage, and $e_{CO_2,ref}$ and $e_{CO_2,CLC}$ are, respectively, the CO_2 emitted per unit electric power of the reference system and of the CLC plant here investigated. Both a natural gas combined cycle (NGCC) plant and a pulverized coal (PC) plant were considered as a reference system. Values of LCOE and CO_2 emission rate assumed are 50 US$ MWh_e^{-1} and 0.379 ton_{CO2} MWh_e^{-1} for the NGCC plant, and 52 US$ MWh_e^{-1} and 0.811 ton_{CO2} MWh_e^{-1} for the PC plant.[1]

The total capital cost of the reactor network was estimated considering the individual costs of the packed bed reactors, OC material, high–temperature valves, turbine, compressors, and steam cycle.

The capital cost of the packed bed reactors was evaluated following the procedure proposed by Hamers et al.[10,24] Reactors are made of an internal refractory, a steel vessel, and an external refractory. The internal refractory insulates the steel vessel from the "hot" OC, and thus protects the vessel from the very high temperature achieved during the OS and HROS. The capital cost of the reactor was then dictated by the mass of the steel and of the internal refractory required, whereas the cost of the external insulating material was considered negligible. Finally, the raw costs were multiplied by the factor of 4 to account for the construction of the reactors. The thickness of the internal refractory was calculated from an energy balance around the reactor wall, using the law of Fourier for thermal conduction

$$Q = \frac{2\pi\lambda L}{\ln\left(\frac{D_a}{D}\right)}\left(T_{max,CLC} - T_{max,steel}\right) \quad (16)$$

where λ is the thermal conductivity of the refractory, L is the length of the reactor, D is the external diameter of the packed bed, D_a is the internal diameter of the reactor plus the internal refractory, $T_{max,CLC}$ is the maximum temperature value achieved during the CLC combustion, and $T_{max,steel}$ is the threshold temperature value set for the steel vessel. Q is the heat loss through the reactor wall, which is assumed to be equal to 0.25% of the energy that would be produced in the combustion of the methane. The diameter of the packed bed is set equal to 0.7 m, while its length to 2.0 m,[32] corresponding to the whole Cu/CuO packed bed for the single-stage configuration and to the sum of the Cu/CuO and Ni/NiO packed beds for the two-stage configuration.

The thickness of the steel vessel (s_{steel}) was calculated as

$$s_{steel} = \frac{pD_a}{4f - 1.5p} \quad (17)$$

where p is the operating pressure, set to 1.5 times the maximum value for safety reason and f is design stress of steel (85 N mm^{-2}). A reference cost of 500 € ton^{-1} was considered for the steel (density of 7850 kg m^{-3}) and of 450 € ton^{-1} for the internal refractory (density of 480 kg m^{-3}). $T_{max,CLC}$ was set at 1173 K for single-stage CLC and 1473 K for two-stage CLC (see Table S1–S2 and/or Figure S1 and S2, Supporting Information), while $T_{max,steel}$ was set at 573 K.

The cost of the high-temperature valves (C_{HTV}) was estimated as[10,24]

$$C_{HTV} = C_{ref,HTV}\left(\frac{V_{max}}{V_{ref}}\right)^{0.6} \quad (18)$$

where V_{max} is the maximum volumetric flow expected at the reactor outlet, $C_{ref,HTV}$ and V_{ref} are the reference cost and reference flowrate value for the high–temperature valve, set equal to 150 000 € and 2 m^3 s^{-1}, respectively. In the economic analysis framework, it is assumed that the use of high-temperature valves is mandatory when the temperature of the exhaust gas equals or exceeds 1000 K.

The OC used in the reactor is a mixture of inert material (alumina) and active phase (Cu/CuO or Ni/NiO). Therefore, its cost was estimated as

$$C_{OC} = 4\{\rho_{OC}[C_{ref,ap}\omega_{ap} + C_{ref,inert}(1-\omega_{ap})]\frac{\pi D^2}{4}L(1-\varepsilon_{bed})\} \quad (19)$$

where ρ_{OC} is the density of the OC, $C_{ref,ap}$ and $C_{ref,inert}$ are the reference cost for the active phase and for the inert, respectively, ω_{ap} is the mass fraction of the active phase in the solid material, and ε_{bed} is the porosity of the packed bed. A factor of 4 was used to account for the synthesis process of the carrier. The reference cost of the active phase was set equal to 6000 and 13 000 € ton^{-1} for, respectively, Cu/CuO and Ni/NiO, according to the average trade price of the pure metals in the last year. The reference cost of the inert material was instead set at 1000 € ton^{-1}.[38]

The cost of the compressors was estimated as[39]

$$C_{comp}[\$] = \frac{39.5\,W_{comp}}{0.9 - \eta_{comp}}\left(\frac{p_{out,comp}}{p_{in,comp}}\right)\ln\left(\frac{p_{out,comp}}{P_{in,comp}}\right) \quad (20)$$

where W_{comp} is the mass flow rate of the stream fed to the compressor, η_{comp} is the efficiency of the compressor, and $p_{out,comp}$ and $p_{in,comp}$ are the outlet and inlet pressure of the compressor,

respectively. The capital cost of the compressor was updated to present value by referring to the chemical engineering plant cost index for the year 2019.

The cost of the gas turbine was estimated as[39]

$$C_{GT}[\$] = \frac{266.3\,W_{GT}}{0.92 - \eta_{GT}}\left(\frac{p_{in,GT}}{p_{out,GT}}\right)[1 + \exp(0.036\,T_{in,GT} - 54.4)] \quad (21)$$

where W_{GT} is the mass flow rate of the stream fed to the turbine, $p_{out,GT}$ and $p_{in,GT}$ are the outlet and inlet pressure of the gas turbine, respectively, and $T_{in,GT}$ is inlet temperature of the stream fed to the gas turbine. As for the compressor, cost of the gas turbine was updated to present value. The capital costs of thermal buffers and the N_2 gas circuit are not considered in this study. Finally, the overall cost of the bottoming steam cycle was evaluated by considering the individual cost of the steam turbine and of the ancillary required components (boiler feedwater pump, heat recovery steam generator, condenser), as detailed in Hanak et al.[33] and updated to present value.

3.2. Results: Comparison of Economic Performance

Table 5 shows the results computed by Equation (2)–(8) for the reactor network featuring two in–parallel fixed beds of set dimensions (2.0 m length, 0.7 m internal diameter). It can be observed that the configuration with two in–series OCs results into higher power production and, thus, better net efficiency. This partly arises from the much higher temperatures achieved during the two–stage CLC (1473 K for two-stage compared with 1173 K for single-stage CLC; see Table S1–S2 and/or Figure S1, S2, Supporting Information). Moreover, the performance of the configuration with the single carrier is further affected by the auxiliary energy required to preheat the input streams. Indeed, about 11% of the electrical energy produced from the gas and steam turbine is required to preheat the air and methane streams up to the required inlet temperature. Compression of the air stream required for both the HROS and OS is by far the most energy intensive process, accounting for about 50–66% of the energy produced. Altogether, for the CLC with a single carrier, the power produced by the reactor network equals 125 kW_e and the plant efficiency is 24.8%. Power production for the two–stage configuration equals to 386 kW_e, with a plant efficiency of 37.2%.

Table 5. Energy performance of the considered reactor networks.

Parameter	Single carrier	Two in–series carriers
E_{GT} [MJ]	1578	586
E_{ST} [MJ]	242	156
$E_{comp,air}$ [MJ]	1194	365
$E_{comp,methane}$ [MJ]	23	14
$E_{aux,air}$ [MJ]	198	–
$E_{aux,methane}$ [MJ]	3	–
P_{net} [kW_e]	125	386
η_{net} [%]	24.8	37.2

Figure 6 shows the total capital costs for the reactor networks designed for the two different configurations. Total capital costs are slightly larger for two–stage CLC, mainly because of the higher temperatures that are achieved within this system. The estimated capital costs are about 548 k€ for the single carrier configuration and 675 k€ for the two carriers configuration, with a difference of about 127 k€. For both scenarios, the high-temperature valves required at the outlet of the reactors account for about 32% of the total costs. Compressors are the second most expensive component, representing about 17–21% of the total capital costs. Actually, the compressors feature the same price for both configurations but represent a lower fraction of the total costs for the two carriers network. Gas and steam turbine represent the third more expensive component, with a share of 14–20% each, followed by the ancillary devices needed by the steam cycle (heat recovery steam generation, boiler feedwater pump, condenser), which account for about 11–13% of capital costs. Finally, packed bed reactors and solid material cumulatively account for 3–4% of the total capital costs.

Figure 7 shows the LCOE for the considered configurations, split in the three main categories of fuel, capital and fixed operating and maintenance costs, variable operating and maintenance costs. The LCOE for the single carrier configuration is

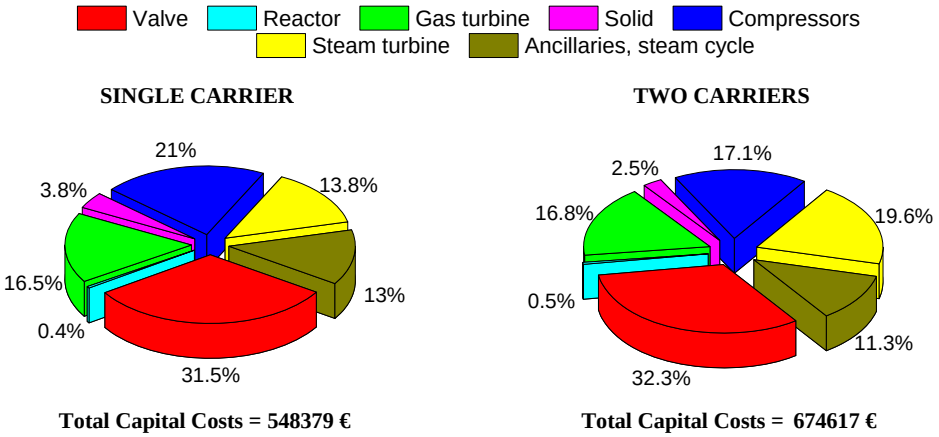

Figure 6. Total capital costs for the considered reactor networks.

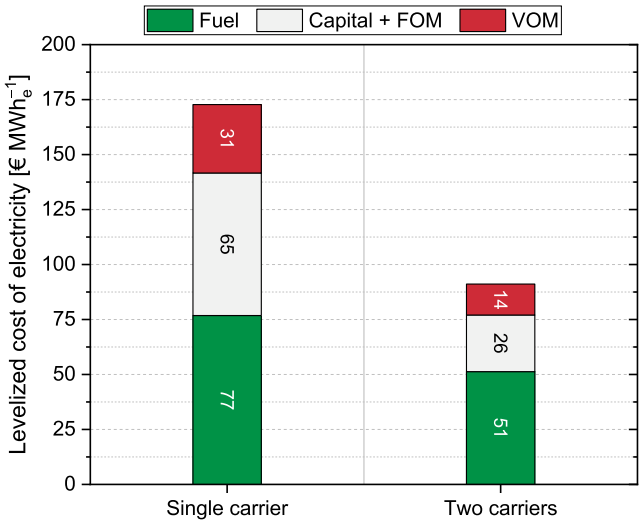

Figure 7. LCOE for the considered reactor networks.

relatively high and amounts to 173 € MWh_e^{-1}, whereas that of the two in–series carriers configuration is considerably smaller and values 91 € MWh_e^{-1}. The price of the fuel and overall efficiency of the plant were shown to be the main contributors to the final value of LCOE. The remarkable difference between the two configurations partly arises from the low efficiency and low power production of the single carrier reactor network. LCOE for the two carriers configuration aligns with that reported by other research groups that assessed the economic viability of CLC in fixed beds.[37]

The costs of the CO_2 avoided were estimated according to Equation (15) and are shown in **Table 6**. As expected, ACC are by far lower for the two–stage CLC. When compared with the NGCC plant, the ACC are higher than those reported in the literature for CLC systems, which are generally smaller than 100 € ton_{CO2}^{-1}.[37,40] This is probably because of the relatively small scale of the plant considered in this study. When compared with a PC plant, the ACC are more than halved, and that of the two OCs configuration aligns with the values reported in the literature for CLC systems.

A sensitivity analysis on the value of LCOE and ACC was subsequently performed by varying individually the reference cost of steam turbine, ancillaries for steam cycle, fuel, compressor, turbine, packed bed reactor, solid reactive material, and high-temperature valves (**Figure 8**). For the readers' convenience, the individual cost of the different components (Table S1, Supporting Information) and the contribution of each item to the final value of LCOE (Table S2, Supporting Information) were reported in the Supporting Information. Analysis of Figure 8 discloses that, for both systems, the fuel price is the main influencing variable. On ±15% variation in this parameter, the values of LCOE and ACC change by ±7% and ±9% for the single carrier configuration, respectively, and by ±8% and ±17% for the two carriers configuration, respectively. The cost of high–temperature valves is the second most influencing component, as a variation of ±15% in their price produces a change of ±3% in LCOE and ±5% in ACC for both configurations. Importantly, for other components, a variation of ±15% in their price affects the values of LCOE and ACC by less than 2%.

Finally, **Figure 9** shows the net present value analysis performed for the considered networks. The analysis discloses the payback period, together with the return on investment, as a function of the sales price of energy with respect to the LCOE. For both cases, the analysis correctly returns a null return on investment after 25 years if the sales price of energy equals the LCOE. With reference to the single carrier configuration, the payback period equals 14, 9, and 6 years after the plant construction for a sales price of energy equal to, respectively, 10%, 25%, and 50% higher with respect to the LCOE. Correspondingly, the return on investment equals 29%, 73%, and 147%. Altogether the investment appears quite risky and has a relatively low return if the energy is not sold at a price at least 50% higher than LCOE. The scenario is more favorable for the two–stage CLC. The payback period is indeed shorter and equals 10, 8, and 5 years after the plant construction for a sales price of energy equal to, respectively, 10%, 25%, and 50% higher with respect to LCOE. The benefits are noticeable also in the return on investment, the corresponding values for which are 39%, 97%, and 194%. When comparing the performances of the considered reactor networks, it should be also kept in mind that the LCOE value for the two carriers configuration is lower. If the same sales price of energy is assumed for the two systems, the advantages of the two carriers configuration become by far larger.

Table 6. ACC for the two reactor configurations.

CLC configuration	ACC [€ ton_{CO2}^{-1}], with reference to	
	NGCC plant	PC plant
Single OC	337	155
Two in–series OCs	122	55

3.3. Discussion

The analysis performed in this study revealed that, within the investigated process conditions, the CLC configuration embodying two in–series OCs performed better than the single carrier one. Despite slightly larger investment costs, the two carriers configuration rewards with smaller values of both LCOE and ACC. Recovery of the sensible heat of the outlet streams for preheating the inlet streams is imperative to reduce the values of LCOE. Moreover, given the intrinsic transient nature of fixed bed reactors, the period of each stage should be carefully designed to synchronize the operation of the different reactors in an integrated parallel scheme. It is here recalled that costs related to the nitrogen required by PS and HRRS were not included in the economic analysis. Assuming that a closed N_2 circuit with a purge/makeup of 5% for PS and 1% for HRRS is used, this would induce an increase in the LCOE of about 31 and 6 € MWh_e for, respectively, the single carrier and two carriers configuration (nitrogen price of 0.05 € m^{-3}). The costs required for the initial purchase of the N_2 would instead be negligible with respect to the values of TCC estimated and shown in Figure 6.

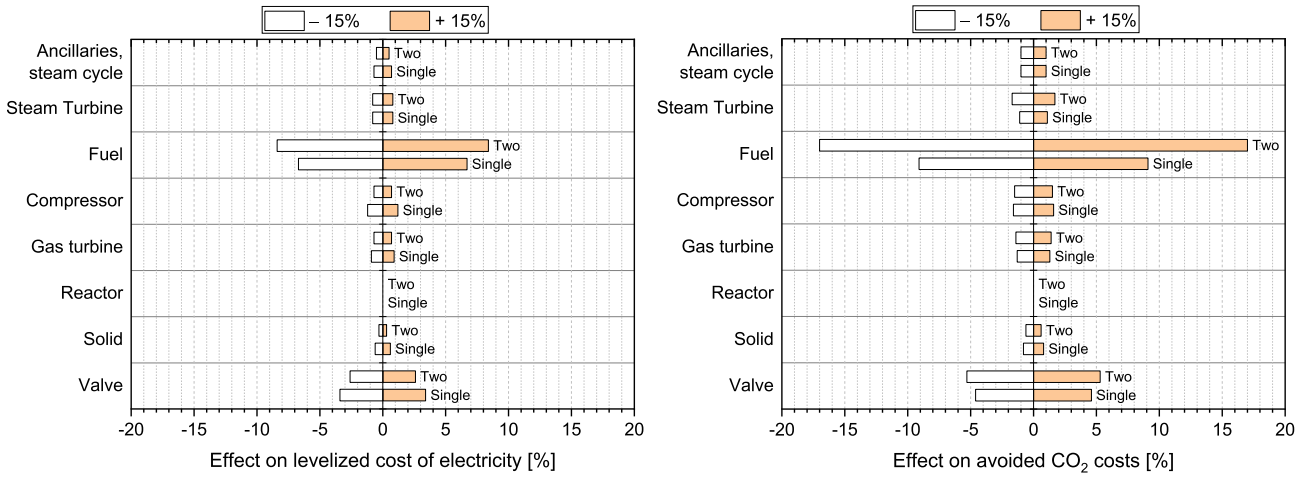

Figure 8. Sensitivity analysis on LCOE and ACC.

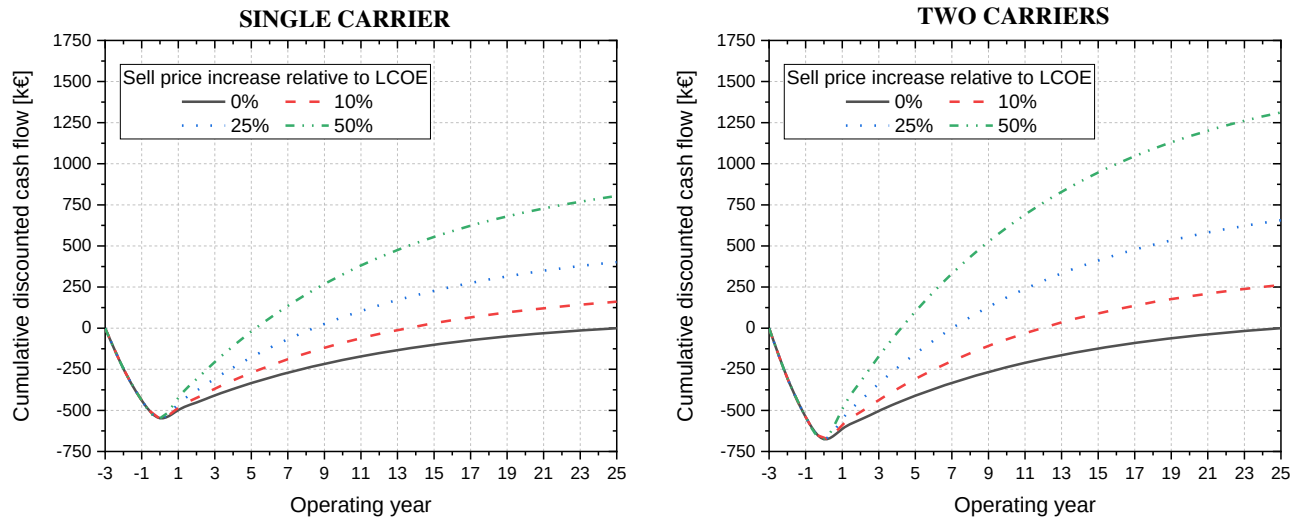

Figure 9. Net present value analysis for the considered reactor networks.

4. Conclusions

A technoeconomic assessment of a chemical looping combustion process in packed bed reactors was performed. Two different configurations were considered, one relying on a single OC (Cu–based) and the other on two in–series OCs (Cu–based first, Ni–based later). For both configurations, relevant process schemes featuring multiple in–parallel reactors, compressors, gas turbine, thermal buffers, and a bottoming steam cycle were devised. Under the considered process conditions, it was observed that a continuous power generation at the turbine could be achieved by using two in–parallel reactors. Importantly, the single carrier configuration required external energy to fulfill preheating of the reactant streams, whereas in the two carriers configuration, exploitation of sensible heat of the exhaust streams was sufficient. The technoeconomic analysis showed that the performance of the two carriers configuration was far better than that of the single carrier configuration. Despite slightly larger capital costs (548 vs 675 k€), the two–stage configuration performed better in terms of efficiency (24.8% vs 37.2%), LCOE (173 vs 91 € MWh_e^{-1}), and ACC (155 vs 55 € ton_{CO2}^{-1}). The sensitivity analysis revealed that the fuel price and high–temperature valves cost are the main influencing variables. The net present value analysis showed that, if energy is sold at 1.5 times the LCOE value, the payback period equals 6 and 5 years for the single- and two-stage configurations, respectively, with a corresponding return on investment of 147% and 194% after 25 years of plant operation. Stimulated by the positive outcomes of this study, future work will include scale–up of the two–stage CLC technology here investigated up to the MW scale.

Supporting Information

Supporting Information is available from the Wiley Online Library or from the author.

Acknowledgements

C.T. wishes to thank the Italian Ministry of University and Research (MUR), for funding his research position within the "PON Ricerca e Innovazione 2014-2020, Asse I Investimenti in Capitale Umano" – AIM 1823125-1, CUP: F84I19000010001.

Open access funding enabled and organized by Projekt DEAL.

Conflict of Interest

The authors declare no conflict of interest.

Data Availability Statement

Data available on request from the authors.

Keywords

CO_2 capture, fixed bed reactors network, oxygen carriers, packed bed, chemical looping combustion

Received: June 21, 2021
Revised: July 22, 2021
Published online: August 12, 2021

[1] B. Metz, O. Davidson, H. de Coninck, M. Loos, L. Meyer, *IPCC, Special Report on Carbon Dioxide Capture and Storage*, Cambridge University Press, Cambridge, UK/New York **2005**.
[2] C. Tregambi, P. Bareschino, E. Mancusi, F. Pepe, F. Montagnaro, R. Solimene, P. Salatino, *Energy Convers. Manag.* **2021**, *230*, 113792.
[3] C. Tregambi, F. Di Lauro, F. Montagnaro, P. Salatino, R. Solimene, *Ind. Eng. Chem. Res.* **2019**, *58*, 21262.
[4] M. Ishida, D. Zheng, T. Akehata, *Energy* **1987**, *12*, 147.
[5] M. Ishida, H. Jin, *Energy* **1994**, *19*, 415.
[6] M. Ishida, H. Jin, US Patent No. 5447024, Tokyo Electric Power Co., Inc., Japan, **1995**.
[7] J. Adánez, L. F. De Diego, F. García-Labiano, P. Gayán, A. Abad, J. M. Palacios, *Energy Fuels* **2004**, *18*, 371.
[8] P. Cho, T. Mattisson, A. Lyngfelt, *Fuel* **2004**, *83*, 1215.
[9] P. Wang, B. Howard, N. Means, *Fuel* **2021**, *285*, 119012.
[10] H. P. Hamers, M. C. Romano, V. Spallina, P. Chiesa, F. Gallucci, M. van Sint Annaland, *Energy* **2015**, *85*, 489.
[11] H. P. Hamers, F. Gallucci, P. D. Cobden, E. Kimball, M. Van Sint Annaland, *Int. J. Greenh. Gas Control* **2013**, *16*, 1.
[12] V. Spallina, M. C. Romano, P. Chiesa, F. Gallucci, M. van Sint Annaland, G. Lozza, *Int. J. Greenh. Gas Control* **2014**, *27*, 28.
[13] S. Cloete, A. Giuffrida, M. Romano, P. Chiesa, M. Pishahang, Y. Larring, *Fuel* **2018**, *220*, 725.
[14] G. Diglio, P. Bareschino, R. Solimene, E. Mancusi, F. Pepe, P. Salatino, *Powder Technol.* **2017**, *316*, 614.
[15] P. Bareschino, E. Mancusi, M. Urciuolo, A. Coppola, R. Solimene, F. Pepe, R. Chirone, P. Salatino, *Powder Technol.* **2020**, *373*, 421.
[16] A. Lyngfelt, B. Leckner, T. Mattisson, *Chem. Eng. Sci.* **2001**, *56*, 3101.
[17] C. Linderholm, A. Abad, T. Mattisson, A. Lyngfelt, *Int. J. Greenh. Gas Control* **2008**, *2*, 520.
[18] C. R. Forero, P. Gayán, L. F. de Diego, A. Abad, F. García-Labiano, J. Adánez, *Fuel Process. Technol.* **2009**, *90*, 1471.
[19] P. Kolbitsch, J. Bolhàr-Nordenkampf, T. Pröll, H. Hofbauer, *Int. J. Greenh. Gas Control.* **2010**, *4*, 180.
[20] V. Spallina, F. Gallucci, M. C. Romano, P. Chiesa, G. Lozza, M. Van Sint Annaland, *Chem. Eng. J.* **2013**, *225*, 174.
[21] S. Noorman, M. Van Sint Annaland, H. Kuipers, *Ind. Eng. Chem. Res.* **2007**, *46*, 4212.
[22] S. Noorman, M. van Sint Annaland, J. A. M. Kuipers, *Chem. Eng. Sci.* **2010**, *65*, 92.
[23] J. Adanez, A. Abad, F. Garcia-Labiano, P. Gayan, L. F. De Diego, *Prog. Energy Combust. Sci.* **2012**, *38*, 215.
[24] H. P. Hamers, M. C. Romano, V. Spallina, P. Chiesa, F. Gallucci, M. V. S. Annaland, *Int. J. Greenh. Gas Control* **2014**, *28*, 65.
[25] J. R. Fernández, J. C. Abanades, *Appl. Energy* **2014**, *135*, 309.
[26] M. Ortiz, F. Gallucci, F. Snijkers, J. Van Noyen, E. Louradour, D. Tournigant, M. van Sint Annaland, *Chem. Eng. J.* **2014**, *245*, 228.
[27] M. Jacobs, J. Van Noyen, Y. Larring, M. McCann, M. Pishahang, S. Amini, M. Ortiz, F. Galluci, M. V. Sint-Annaland, D. Tournigant, E. Louradour, F. Snijkers, *Appl. Energy* **2015**, *157*, 374.
[28] H. P. Hamers, F. Gallucci, G. Williams, P. D. Cobden, M. Van Sint Annaland, *Energy Fuels* **2015**, *29*, 2656.
[29] L. Han, G. M. Bollas, *Energy* **2016**, *102*, 669.
[30] M. Lucio, L. A. Ricardez-Sandoval, *Fuel* **2020**, *262*, 116544.
[31] R. F. Kooiman, H. P. Hamers, F. Gallucci, M. Van Sint Annaland, *Ind. Eng. Chem. Res.* **2015**, *54*, 2001.
[32] E. Mancusi, P. Bareschino, A. Forgione, F. Pepe, *Int. J. Greenh. Gas Control* **2020**, *99*, 103099.
[33] D. P. Hanak, B. G. Jenkins, T. Kruger, V. Manovic, *Appl. Energy* **2017**, *205*, 1189.
[34] N. Khallaghi, D. P. Hanak, V. Manovic, *Appl. Energy*. **2019**, *249*, 237.
[35] V. Spallina, G. Motamedi, F. Gallucci, M. van Sint Annaland, *Int. J. Greenh. Gas Control* **2019**, *88*, 71.
[36] S. Michalski, D. P. Hanak, V. Manovic, *J. Clean. Prod.* **2019**, *219*, 540.
[37] L. Mancuso, S. Cloete, P. Chiesa, S. Amini, *Int. J. Greenh. Gas Control* **2017**, *64*, 223–233.
[38] G. Diglio, P. Bareschino, E. Mancusi, F. Pepe, F. Montagnaro, D. P. Hanak, V. Manovic, *Appl. Energy* **2018**, *230*, 241.
[39] A. Valero, M. A. Lozano, L. Serra, G. Tsatsaronis, J. Pisa, C. Frangopoulos, M. R. von Spakovsky, *Energy* **1994**, *19*, 279.
[40] S. Cloete, A. Tobiesen, J. Morud, M. Romano, P. Chiesa, A. Giuffrida, Y. Larring, *Int. J. Greenh. Gas Control* **2018**, *78*, 354.